

Room temperature cost-effective synthesis of carbon quantum dots for fluorescent pattern recognition of metal ions

Yifan Lu,^a Wenbang Yu,^b Guoyue Shi,^a Min Zhang^{a*}

^aSchool of Chemistry and Molecular Engineering, Shanghai Key Laboratory for Urban Ecological Processes and Eco-Restoration, East China Normal University, Dongchuan Road 500, Shanghai 200241, China.

^bJinhua Polytechnic, Jinhua 321000, Zhejiang Province, China.

Experimental Section

Reagents and Materials

o-phthalaldehyde (OPA) and quinine sulfate were purchased from Aladdin. Polyethyleneimine (PEI) ($M_w=600$) was purchased from Adamas-beta Co. Ltd (Shanghai, China). The following metal salts, CuCl_2 , CoCl_2 , NiCl_2 , MnCl_2 , CrCl_3 , FeCl_3 , FeCl_2 , MgCl_2 , AlCl_3 , $\text{Zn}(\text{NO}_3)_2$, $\text{Pb}(\text{NO}_3)_2$ were obtained from Sinopharm Chemical Reagent Co. Ltd. (Shanghai, China). $\text{Hg}(\text{NO}_3)_2$ reference material was purchased from Titan Scientific Co. Ltd. (Shanghai, China). Tris-(hydroxymethyl)-aminomethane (Tris) was purchased from Sangon Biotech Co. Ltd. (Shanghai, China). Among these reagents, quinine sulfate was biological reagent grade, Tris was molecular biology grade and all other reagents were analytical reagent grade. All chemicals listed above were used without any further purification. Ultrapure water ($\geq 18 \text{ M}\Omega\text{-cm}$) was generated by Hitachi water purification system (Shanghai, China) and used throughout the experiments.

Synthesis of CDs

The OP-CDs were synthesized at room temperature without consuming energy and additional reagents. 0.24 g OPA was dissolved in 10 mL water under ultrasound (under low temperature conditions in case oxidating) and 0.54 g PEI was dissolved in 15 mL water. The two solutions were combined by stirring at room temperature after being thoroughly dissolved. Several minutes later, from being colorless and clear, the mixed solution turned orange, which proofed the progression of the Schiff Base reaction. The reaction ceased after 45 minutes and the precipitate was eliminated though filtration, leaving just the supernatant. Then the supernatant was transferred to a dialysis membrane (molecular weight of 1000 Da) for dialysis against water, sustaining 12 h during which water was changed every 3 h. The post-processed solution exhibited strong yellow-green luminescence under the 365 nm UV light lamp (Fig. S1†). The purified solution was then lyophilized and stored at 4 °C for further use.

Fluorescent Assay of Metal Ions by OP-CDs Sensor Array

Tris-HCl buffer (10 mM) was prepared by dissolving Tris in water and adjusting pH to 6,7,8 respectively by 0.1 M HCl in advance. OP-CDs were reconfigured into 0.5 mg/mL and all metal ions were dissolved in water on demand. Then 10 μL OP-CDs, 10 μL metal ions and 80 μL Tris-HCl buffer were added to the 384-well black microplate, after thoroughly mixing. Metal ions bound to OP-CDs, changing the intensity of the fluorescence, which revealed different change amplitude in different buffers. The fluorescence change could be used to describe the effect of metal ions on OP-CDs, which was defined as $(F - F_0)/F_0$, where F_0 and F were the fluorescence intensity of 490 nm excited at 426 nm in the absence and presence of metal ions. Each combination between metal ions and OP-CDs had five parallel replicates. The raw data matrix (3 Tris-HCl buffers \times 12 metal ions \times 5 replicates) was collected and further analyzed by principal component analysis (PCA) through using SPSS 22.0 software (IBM) and the data plotting was depicted in GraphPad Prism 8.3.0 software.

Characterization

Fluorescence measurements were carried out through a TECAN microplate reader (infinite M200 pro) and all fluorescence measurements were proceeded with a 384-well black microplate. UV-visible absorption spectroscopy was recorded by a UV-visible spectrophotometer. The fluorescence lifetime was characterized with an Edinburgh fluorescence spectrometer (FLS980). Transmission electron microscope (TEM) images were collected on a field emission transmission electron microscope (TECNAI G2F20). Also, the average size of OP-CDs was calculated by analyzing the average size of 150 single CDs (Nano Measurer 1.2 software). Fourier transform infrared spectroscopy (FTIR) was obtained by using a Nicolet optical bench (Nexus 670). X-ray photoelectron spectroscopy (XPS) data was acquired by Thermo Fisher Scientific (Escalab 250Xi). Dynamic light scattering (DLS) data was gained through a Malvern Zetasizer Nanoseries (ZS90).

Measurement of quantum yield (QY) of OP-CDs

The QY of OP-CDs was measured and calculated in both neutral environment of water and acidic environment of H_2SO_4 through the fluorescence method using quinine sulfate ($\Phi = 0.54$) as a standard fluorophore. Five different concentrations of quinine sulfate were dissolved in 0.1 M H_2SO_4 and five different concentrations of OP-CDs were dissolved in water and 0.1 M H_2SO_4 respectively. Then, the UV-visible absorption spectrum and fluorescence spectrum of each solution was recorded. The absorbance could be obtained directly from spectrum and corresponding fluorescence curve areas were calculated using Origin 2019 software.

Supplementary Figures

Fig. S1 The optical photograph of OP-CDs. (a) the optical images under daylight (b) the optical images under the 365 nm UV light lamp.

Fig. S2 Histograms and Gauss fittings of particle size distribution of OP-CDs.

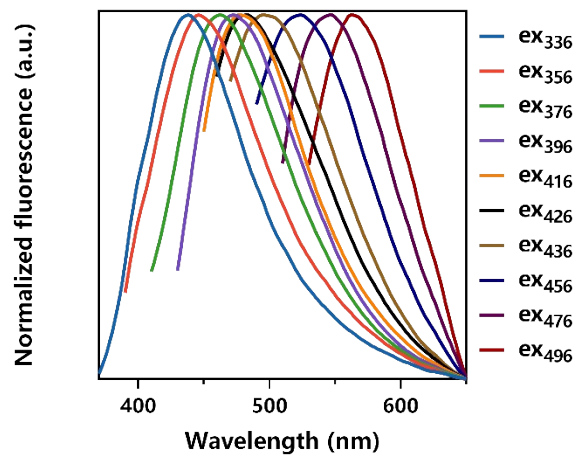


Fig. S3 Normalized emission spectra of OP-CDs with increasing excitation wavelength from 336 nm to 496nm.



Fig. S4 Photos of OP-CDs in different pH solutions, with pH increasing from left to right (1-9).

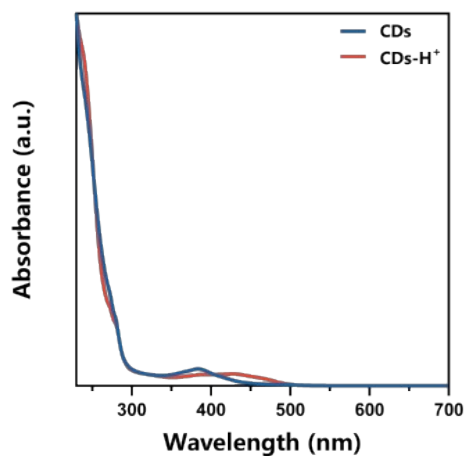


Fig. S5 UV absorption spectrum of OP-CDs in neutral and acidic conditions respectively.

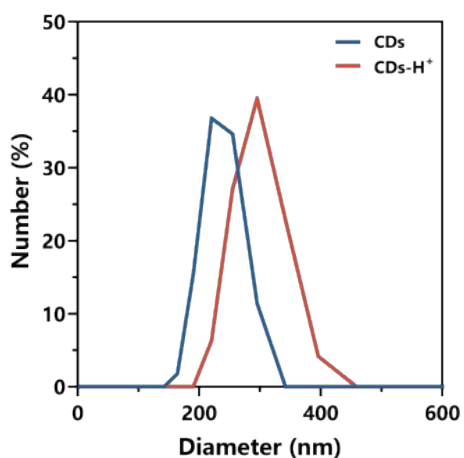


Fig. S6 Particle sizes of OP-CDs in neutral and acidic conditions respectively.

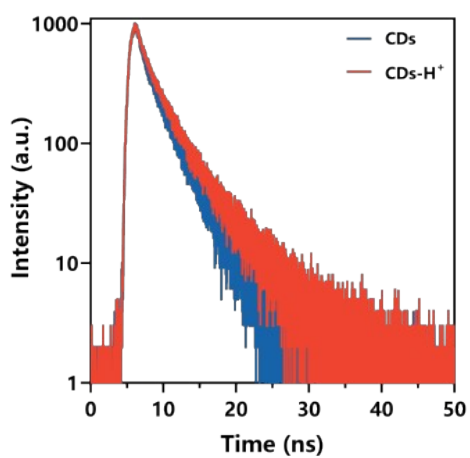


Fig. S7 Fluorescence lifetime curves of OP-CDs in neutral and acidic conditions respectively, with excitation wavelength at 426 nm.

Fig. S8 The linear relationship between fluorescence curve areas and absorbance of (a) OP-CDs in neutral environment, (b) OP-CDs in acidic environment and (c) quinine sulfate.

Table S1 Comparison of reaction time, source of carbon, QY, reaction condition and extra reagents of room-temperature synthesized CDs.

Reaction time	Source of carbon	QY	Reaction condition and extra reagents	Document
Overnight	PEG	1.95%	4M NaOH R. T.	[1]
Overnight	Phenol/formaldehyde resins	10–15%	Amphiphilic triblock copolymer R. T.	[2]
12 h	Resorcinol EDA	12.0%	NaH ₂ PO ₄ R. T.	[3]
20 h	TETA PBQ	35.3%	R. T.	[4]
3 h	Glyoxal OPD	Not mentioned	R. T.	[5]
45 min	PEI OPA	38.64%/ 4.76%	R. T.	This work

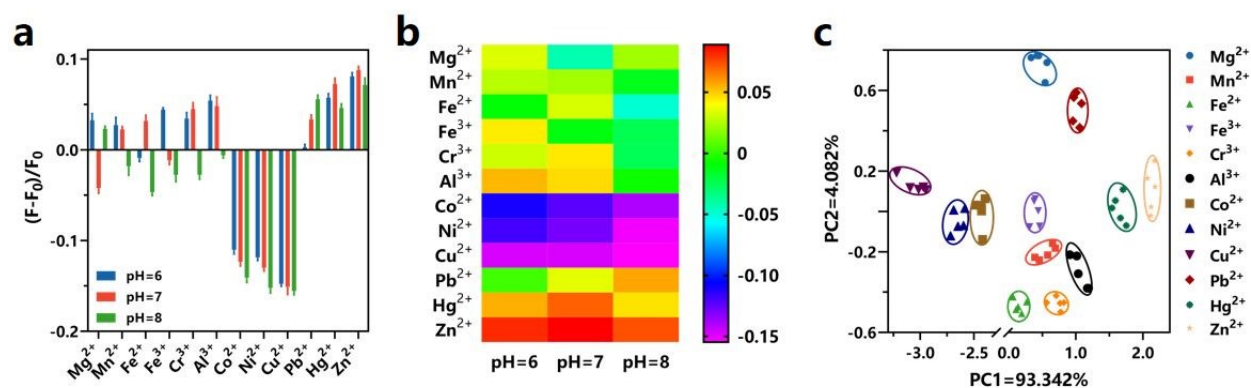


Fig. S9 The discrimination for metal ions of OP-CDs sensor array in low concentration. (a) Fluorescence response patterns of OP-CDs toward 12 metal ions (10 μ M) in Tris buffers with three different pH. (b) Heat map derived from fluorescence response patterns of OP-CDs. (c) 2D PCA scatter plot of OP-CDs towards metal ions indicated.

Table S2 Comparison of linear detection range, LOD and R² of CDs for metal ions detection.

Fluorescent probe	Metal ions detected	linear detection range	LOD	R ²	Documents
Diethylenetriamine- β -cyclodextrin-modified CDs	Hg ²⁺	0–87 μ M	0.25 μ M	0.999	[6]
	Fe ³⁺	0–140 μ M	0.57 μ M	0.994	
Hetero atom doping CDs	Hg ²⁺	0–12 μ M	0.23 μ M	0.992	[7]
CDs from rose-heart radish	Fe ³⁺	0.02–40 μ M	0.13 μ M	0.993	[8]
OP-CDs	Cu ²⁺	1–60 μ M	0.43 μ M	0.997	This work
	Hg ²⁺	1–80 μ M	0.62 μ M	0.991	

Zn²⁺

1–40 μM

0.76 μM

0.992

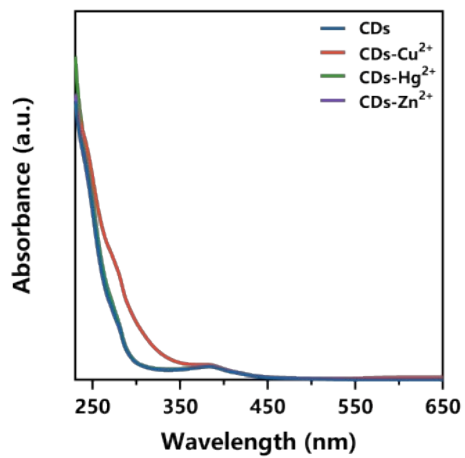


Fig. S10 UV absorption spectrum of OP-CDs with Cu²⁺, Hg²⁺ and Zn²⁺.

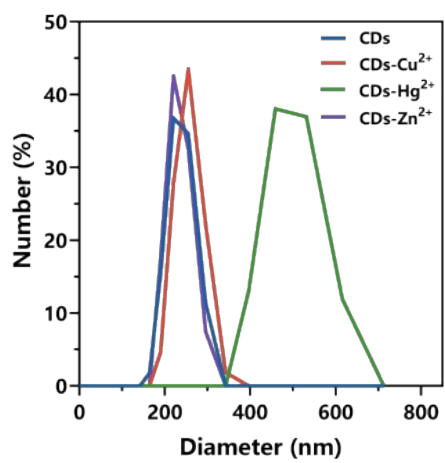


Fig. S11 Particle sizes of OP-CDs with Cu²⁺, Hg²⁺ and Zn²⁺.

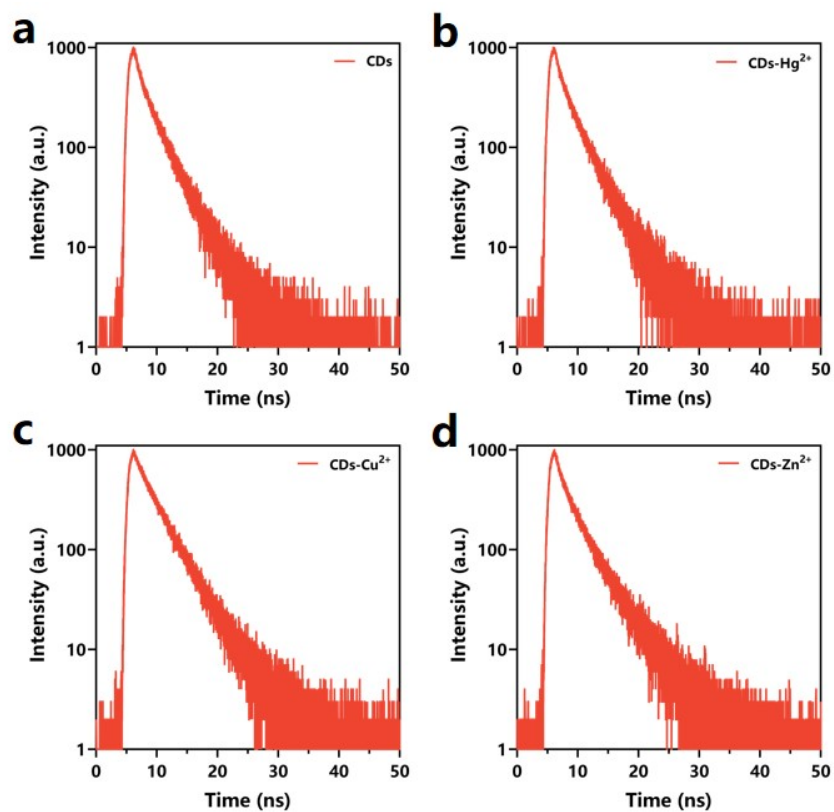


Fig. S12 Fluorescence lifetime curves of (a) OP-CDs and OP-CDs with (b) Hg²⁺, (c) Cu²⁺ and (d) Zn²⁺ with excitation wavelength at 426 nm.

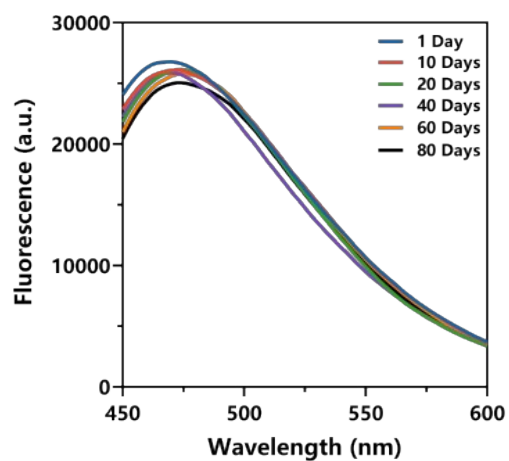


Fig. S13 Emission spectra of OP-CDs for 80 days.

References

- 1 S. Mitra, S. Chandra, S. H. Pathan, N. Sikdar, P. Pramanik and A. Goswami, *RSC Adv.*, 2013, 3, 3189-3193.
- 2 R. Liu, D. Wu, S. Liu, K. Koynov, W. Knoll and Q. Li, *Angew. Chem. Int. Ed.*, 2009, 48, 4598-4601.
- 3 C. Yu, X. Li, X. Qiao, Z. Zhang, D. Zhang, H. Liu, X. L. Hao, Z. Wang, H. You and L. Zhou, *J. Phys. Chem. C*, 2023, 127, 3176-3183.
- 4 M. L. Liu, L. Yang, R. S. Li, B. B. Chen, H. Liu and C. Z. Huang, *Green Chem.*, 2017, 19, 3611-3617.
- 5 Y. Yan, J. H. Liu, R. S. Li, Y. F. Li, C. Z. Huang and S. J. Zhen, *Anal. Chim. Acta*, 2019, 1063, 144-151.
- 6 J. Yang, Y. Yang, L. Su, X. Tao, J. Zhang, Y. Chen and L. Yang, *Spectrochim. Acta A*, 2023, 291, 122364.
- 7 F. Yan, Y. Zou, M. Wang, X. Mu, N. Yang and L. Chen, *Sensor Actuat. B-Chem.*, 2014, 192, 488-495.
- 8 W. Liu, H. Diao, H. Chang, H. Wang, T. Li and W. Wei, *Sensor Actuat. B-Chem.*, 2017, 241, 190-198.